Macromolecules
Cite This: Macromolecules XXXX, XXX, XXX–XXX
Article
pubs.acs.org/Macromolecules

Tailorable Degradation of pH-Responsive All-Polyether Micelles: Unveiling the Role of Monomer Structure and Hydrophilic–Hydrophobic Balance

Eunbyul Hwang,[†,‡,§] Kicheol Kim,[‡] Chae Gyu Lee,[‡] Tae-Hyuk Kwon,[‡] Sang-Ho Lee,*[,§] Seung Kyu Min,*[,‡] and Byeong-Su Kim*[,†]

[†]Department of Chemistry, Yonsei University, Seoul 03722, Republic of Korea
[‡]Department of Chemistry, Ulsan National Institute of Science and Technology (UNIST), Ulsan 44919, Republic of Korea
[§]Research Center for Green Fine Chemicals, Korea Research Institute of Chemical Technology, Ulsan 44412, Republic of Korea

Supporting Information

ABSTRACT: Polymeric micelles have been widely used as ideal drug-delivery vehicles with unique advantages. However, fine tuning of the degradation rates of micelles over a wide time frame remains challenging. Herein, we designed and synthesized a novel pH-responsive, hydrophobic epoxide monomer, tetrahydrofuranyl glycidyl ether (TFGE), carrying an acetal group as a cleavable linkage. The hydrolysis kinetics of TFGE was carefully evaluated with representative functional epoxide monomers, such as 1-ethoxyethyl glycidyl ether and tetrahydropyranyl glycidyl ether, via in situ ^{1}H NMR spectroscopy and quantum mechanical calculations. Interestingly, the hydrolysis kinetics and the associated energy barrier were closely related not only to the cyclic/acyclic structure of the monomers but also to their hydrophobicity. Subsequently, a series of amphiphilic block copolymers (*m*PEG-*b*-PTFGE) were synthesized via anionic ring-opening polymerization and the self-assembled polymeric micelles were evaluated with respect to critical micelle concentration, encapsulation efficiency, drug release, and cell viability. Most notably, the release kinetics of the model compound from polymeric micelles exhibited a different trend, confirming the critical role of hydrophobicity in governing the pH-responsive hydrolysis of the polymeric micelles. This study provides new insights applicable to the design of functional monomers for tailoring the release profiles of polymeric micelles for smart drug delivery.

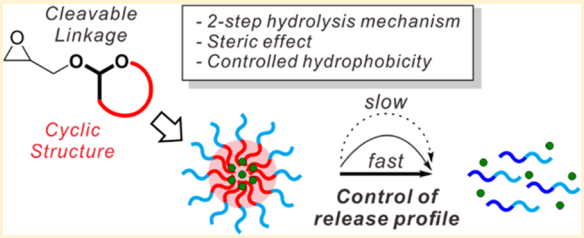

INTRODUCTION

A drug-delivery system is a means of transporting pharmaceutical compounds safely and efficiently in the body. There have been significant advances involving various nanoscale carriers for effective drug delivery, including nanogels,[1] liposomes,[2] and micelles.[3] Among these, polymeric micelles using amphiphilic block copolymers have garnered particular attention owing to their high drug-loading capacity and high stability in the bloodstream.[4] Moreover, the high chemical tunability of each monomer block enables tailoring of the stability and functionality of the resulting self-assembled nanostructure. In particular, there have been significant endeavors in tuning the release profiles of the active therapeutics in drug-delivery system by controlling various aspects, especially of the hydrophobic block of the polymeric micelles, including molecular weight,[5] substituents,[6] stereoregularity,[7] and crystallinity.[8,9] In addition, self-assembled hydrophobic cores with specific chemical functionality responsive to various biological stimuli such as redox, temperature, light, and pH have been designed to deliver therapeutic agents in a site-specific and time-controlled manner through smart drug-delivery systems.[10,11]

Over the past few years, on the other hand, efforts have been directed to introduce cleavable linkages into the hydrophobic blocks in polymer chains to induce specific degradation behaviors for efficient control of drug-release profiles. As one representative example, pH-responsive micelles containing acid-degradable linkages provide facile access to site-specific delivery of the therapeutics, as the linkages are hydrolyzed upon entering the cytosol of acidic cancer cells. Among the various degradable linkages,[12,13] such as hydrazones, imines, carbonates, and acetals, the acetal linkages possess particular benefits for biomedical applications owing to the generation of nontoxic and soluble byproducts after cleavage, affording facile renal clearance from the body. For example, Endo and co-workers studied the feasibility of self-assembly and degradation behavior of amphiphilic copolymers using a new acrylate-based cleavable monomer in the hydrophobic block.[14] Kizhakkedathu and co-workers developed branched degradable polyethers with structurally varying ketal groups and studied their degradation kinetics based on their hydrophobicity.[15] More

Received: April 21, 2019
Revised: June 25, 2019

DOI: 10.1021/acs.macromol.9b00823
Macromolecules XXXX, XXX, XXX–XXX

Scheme 1. Structural Design of Epoxide Monomers Carrying Cyclic Pendant Groups for Advanced Polymeric Micelle Release Profile via Cooperative Degradation

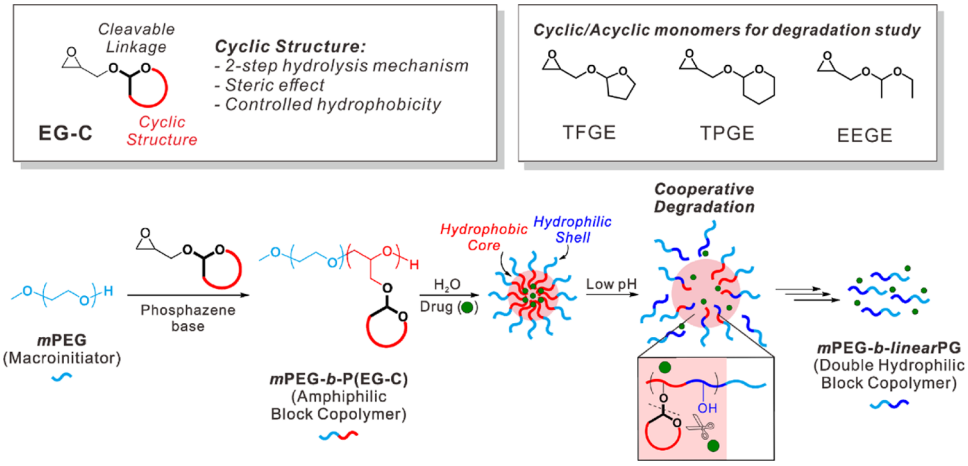

recently, Zhong and co-workers have reported amphiphilic triblock copolymer micelles for a pH-sensitive intracellular drug-delivery system using poly(acetal urethane) as the hydrophobic block.[16] The release profiles of the micelles for different block lengths of poly(acetal urethane) under various pH conditions were investigated. Furthermore, we have recently reported a novel functional epoxide monomer carrying an acetal-cleavable linkage as the hydrophobic block in a pH-responsive drug-delivery system. The self-assembly of amphiphilic block copolymers into a micelle and its degradation kinetics under acidic conditions compared to other block copolymers were carefully examined.[17]

Despite the successful control of the degradation kinetics of polymeric micelles, however, it is still highly desirable to correlate the structural design of functional monomers with that of the hydrophobic block of polymeric micelles, as the degradation kinetics of polymeric micelles are dependent on multiple parameters, including structure of cleavable groups, hydrophobicity, and steric effects within the micelle.

Our strategy is to design a new epoxide monomer with a cyclic structure at the pendant group with an acetal moiety as a cleavable linkage (EG-C). Such a cyclic pendant group of the monomer would affect the hydrolysis rate owing to steric effect and controlled hydrophobicity. The phosphazene-based anionic ring-opening polymerization (AROP) from poly(ethylene glycol) methyl ether (*m*PEG) as a macroinitiator affords a series of well-defined amphiphilic block copolymers (*m*PEG-*b*-P(EG-C)). These block copolymers generate a polymeric micelle in water, which can be cooperatively degraded by cleaved pendant groups on the hydrophobic core at low pH, providing biocompatible double hydrophilic block copolymers, *m*PEG-*b*-linear polyglycerol (*m*PEG-*b*-linear PG) (Scheme 1).

Previously, our group studied degradation kinetics of amphiphilic copolymer micelles with pH-responsive epoxide monomers, 1-ethoxyethyl glycidyl ether (EEGE; acyclic) and tetrahydropyranyl glycidyl ether (TPGE; cyclic, 6-membered ring).[17,18] The micelle composed of *m*PEG-*b*-PTPGE copolymer showed a significantly lower degradation rate than *m*PEG-*b*-PEEGE, which was attributed to the hydrophobicity and the rigidity of TPGE monomer. Thus, in this study, we extended a step further to enrich the selection of the monomer library in the controlled drug delivery. Herein, we prepared the novel pH-responsive cyclic structure of a hydrophobic epoxide monomer, tetrahydrofuranyl glycidyl ether (TFGE; cyclic, 5-membered ring). We anticipate that TFGE would be hydrolyzed in an intermediate rate because of the presence of cyclic moiety but with less hydrophobicity.

Moreover, the quantum mechanical (QM) calculations suggest a new mechanism for hydrolysis and identifying factors that critically affect the hydrolysis kinetics of micelles, that is, the cyclic/acyclic structure and the hydrophobicity/hydrophilicity of the monomers (Scheme 1). Also, the corresponding amphiphilic block copolymer micelles are evaluated in relation to existing pH-responsive epoxide monomers, EEGE and TPGE. All of these polyether-based micelles are anticipated to expand the variety of approaches to achieving site-specific and time-controlled smart drug-delivery systems.

EXPERIMENTAL SECTION

Materials and Reagents. Glycidol (Sigma-Aldrich; 96%) and ethyl vinyl ether (Sigma-Aldrich; contains 0.1% KOH as stabilizer, 99%) were stored at 0 °C before use. 1-Propanol (Sigma-Aldrich; >99.5%), 2,3-dihydrofuran (Thermo Fisher Scientific; >98%), 3,4-dihydro-2*H*-pyran (Sigma-Aldrich; 97%), *p*-toluenesulfonic acid monohydrate (*p*-TsOH, Sigma-Aldrich; >98%), phosphazene base P_4-*t*-Bu solution (*t*-Bu-P_4, Sigma-Aldrich; ∼0.8 M in hexane), benzoic acid (Sigma-Aldrich; 99.5%), toluene (Thermo Fisher Scientific; anhydrous, 99.8%, over molecular sieves, packaged under argon), and pyrene (Sigma-Aldrich; >99%) were used as received. Poly(ethylene glycol) methyl ether (*m*PEG, Sigma-Aldrich; average M_n, 5000) was dried by azeotropic distillation with the addition of toluene. Benzyl alcohol (BnOH, Sigma-Aldrich; anhydrous, 99.8%) was dried over molecular sieves 4A. The deuterated NMR solvents, $CDCl_3$ and D_2O, were purchased from Cambridge Isotope Laboratories, Inc. The deuterated sodium acetate/acetic acid buffer was made of sodium acetate-d_3 (Cambridge Isotope Laboratories, Inc; 99%) and acetic acid-d_4 (Cambridge Isotope Laboratories, Inc; 98%).

Characterization. ^{1}H NMR (400 MHz) and ^{13}C NMR (100 MHz) spectra were acquired using an AVANCE III HD NMR spectrometer (Bruker). All spectra were recorded in ppm with the deuterated solvents, D_2O and $CDCl_3$. Gel permeation chromatography (GPC) measurements (Agilent 1200 series) were performed in $CHCl_3$ as an eluent at 25 °C at a flow rate of 1.0 mL min^{-1} using a refractive index (RI) detector. Standard poly(methyl methacrylate) samples were used for calibration to determine the number (M_n)- and weight (M_w)-average molecular weights and molecular weight distribution (M_w/M_n). Matrix-assisted laser desorption and ionization time-of-flight (MALDI-TOF) mass spectrometry was performed using

DOI: 10.1021/acs.macromol.9b00823
Macromolecules XXXX, XXX, XXX−XXX

Table 1. Characterization Data for All Polymers Used in This Study

polymer code[a]	polymer composition	conversion[b]	$M_{n,NMR}$[b] (g mol^{-1})	$M_{n,GPC}$[c] (g mol^{-1})	M_w/M_n[c]	T_g[d] (°C)	CMC[e] (mg L^{-1})
H32	$PTFGE_{32}$	>99%	4700	3800	1.08	−24	n/d
H42	$PTFGE_{42}$	>99%	6200	4500	1.08	−24	n/d
F11	$m PEG_{114}$-*b*-$PTFGE_{11}$	>99%	6600	11 600	1.05	−35	626.7
F30	$m PEG_{114}$-*b*-$PTFGE_{30}$	>99%	9300	13 500	1.06	−29	150.6
F47	$m PEG_{114}$-*b*-$PTFGE_{47}$	>99%	11 800	15 300	1.07	−28	113.6
P27[f]	$m PEG_{114}$-*b*-$PTPGE_{27}$	>99%	9300	12 300	1.03	−18	10.9
E27[f]	$m PEG_{114}$-*b*-$PEEGE_{27}$	>99%	8900	14 300	1.03	−59	76.7

[a]The letters H, F, P, and E and the number indicate the homopolymer, *m*PEG-*b*-PTFGE, *m*PEG-*b*-PTPGE, *m*PEG-*b*-PEEGE, and the degree of polymerization, respectively. [b]Determined via ^{1}H NMR spectroscopy. [c]Measured by GPC ($CHCl_3$, RI signal, PMMA standard). [d]T_g was determined by DSC at a rate of 10 °C min^{-1}. [e]Critical micelle concentration (CMC) value was calculated from fluorescence spectroscopy using pyrene as a probe. [f]The polymers were described in a previous paper.[18]

an Ultraflex III MALDI mass spectrometer with 2,5-dihydroxybenzoic acid as the matrix. Differential scanning calorimetry (DSC) (Q200 model, TA Instruments) was carried out under a nitrogen atmosphere in a temperature range of −80−65 °C and at a heating rate of 10 °C min^{-1}. Critical micelle concentration (CMC) measurements, determination of encapsulation efficiency with Nile Red, and the release profile of pyrene were obtained using a fluorimeter (RF-6000, Shimadzu). Dynamic light scattering (DLS, SZ-100, HORIBA) measurements were performed using a nanoparticle analyzer equipped with a solid-state laser (λ = 532 nm). The intensity autocorrelation function was measured at an angle of 90 °C. The morphology and the size of the micelles were investigated using atomic force microscopy (AFM, Park System, NX-10) via a noncontact mode.

Synthesis of the Tetrahydrofuranyl Glycidyl Ether (TFGE) Monomer. A solution of glycidol (19.6 g, 0.264 mol) and 2,3-dihydrofuran (25.0 g, 0.357 mol) in dichloromethane (300 mL) was introduced into a round-bottom flask and stirred at 0 °C for 30 min. To this solution, *p*-toluenesulfonic acid (1.36 g, 7.92 mmol) was slowly added, followed by stirring for 8 h at room temperature. The solution was stirred for additional 1 h after the addition of saturated $NaHCO_3$ solution. The aqueous phase was extracted with dichloromethane, and the organic layers were extracted with deionized water. The combined organic layers were dried over Na_2SO_4. The organic phase was concentrated under reduced pressure, and the residue was purified by fractional distillation to obtain 27.5 g (75%) of the TFGE monomer; this was confirmed by various characterization techniques, including ^{1}H and ^{13}C NMR, correlation spectroscopy (COSY), heteronuclear single-quantum correlation (HSQC), electrospray ionization mass spectrometry (ESI-MS), and gas chromatography−mass spectrometry (GC−MS) (see Figure 3 for corresponding peak assignments and Figures S6−S10 in the Supporting Information). ^{1}H NMR (400 MHz, chloroform-*d*) δ 5.16 (ddd, J = 8.7, 3.2, 2.3 Hz, 1H), 3.97−3.82 (m, 2H), 3.65 (d, J = 4.3 Hz, 1H), 3.34 (dd, J = 11.6, 6.6 Hz, 1H), 3.19−3.10 (m, 1H), 2.80 (ddd, J = 5.1, 4.1, 2.2 Hz, 1H), 2.61 (ddd, J = 21.8, 5.1, 2.7 Hz, 1H), 2.08−1.76 (m, 4H). ^{13}C NMR (101 MHz, chloroform-*d*) δ 104.03, 103.99, 68.26, 67.10, 66.94, 66.93, 50.86, 50.46, 44.50, 44.48, 32.23, 32.21, 23.27, 23.26.

Representative Procedure of Homopolymerization. A 0.22 mL solution of *t*-BuP_4 (0.80 M, 0.174 mmol) in *n*-hexane was added to a solution of benzyl alcohol (18.0 μL, 0.174 mmol) in toluene under an argon atmosphere. TFGE (1.0 g, 6.94 mmol) was then added to the solution dropwise using a syringe pump to initiate the polymerization over 6 h. After stirring at room temperature for 24 h, the polymerization was quenched by the addition of benzoic acid (31.9 mg, 0.261 mmol). After precipitation in hexane, the mixture was passed through an alumina pad using dichloromethane. The polymer solution was then evaporated to dryness to obtain PTFGE (270 mg) (yield: 27%). The molecular weight of PTFGE (H42 in Table 1) was 6200 g mol^{-1}, as calculated from the NMR data shown in Figure 3 using the following equation: number of repeating units (TFGE) = 42 (integration value of methine peak, 42H, 5.10 ppm, and methylene of benzyl alcohol, 2H, 4.54 ppm); M_n = 144.17 g mol^{-1} (molecular weight of the TFGE monomer) × 42 (number of repeating units) + 108.14 g mol^{-1} (molecular weight of benzyl alcohol) = 6163.28 g mol^{-1}. Considering the error range of NMR integration, we used 6200 g mol^{-1} as the M_n value of the PTFGE. ^{1}H NMR (400 MHz, chloroform-*d*) δ 7.34−7.31 (m, 4H), 5.10 (s, 42H), 4.54 (s, 2H), 3.99−3.26 (m, 315H), 2.11−1.67 (m, 178H).

Representative Procedure of Block Copolymerization. Block copolymer synthesis was conducted using poly(ethylene glycol)-methyl ether (*m*PEG) as a macroinitiator. *m*PEG (0.5 g, 0.10 mmol, 0.025 M) was placed in a flask under an argon flow. Toluene (3.0 mL) was then added into the flask, and the mixture was stirred for 30 min at 60 °C. After cooling to room temperature, 0.13 mL of *t*-BuP_4 in *n*-hexane (0.8 M, 0.10 mmol) was added to the solution. Then, TFGE (0.87 g, 6.0 mmol, 1.5 M) was added to the solution dropwise using a syringe pump for 6 h. After stirring at room temperature for 24 h, the polymerization was terminated by the addition of benzoic acid (0.037 g, 0.30 mmol). After precipitation in hexane, the reaction mixture was passed through a pad of alumina with dichloromethane. The solution was evaporated to dryness to give F47 (Table 1; 370 mg) (yield: 27%). The molecular weight of F47 was determined to be 11 800 g mol^{-1}, as calculated from the NMR data (Figure 3) using the following equation: number of repeating units (TFGE) = 47 (integration value of methine peak, 47H, 5.10 ppm, and methyl of *m*PEG, 3H, 3.37 ppm); M_n = 144.17 g mol^{-1} (molecular weight of the TFGE monomer) × 47 (number of repeating units) + 5000 g mol^{-1} (molecular weight of *m*PEG) = 11 775.99 g mol^{-1}. Considering the error range of NMR integration, we used 11 800 g mol^{-1} as the M_n value of the F47. ^{1}H NMR (400 MHz, chloroform-*d*) δ 5.10 (m, 47H), 3.93−3.38 (s, 1098H), 3.37 (s, 3H), 2.04−1.73 (m, 224H).

Measurement of CMC Using Pyrene Fluorescence. A series of polymer solutions in dimethylformamide (DMF) at various concentrations were prepared. A 10 μL solution of pyrene (5.2 mg L^{-1} in DMF) was added to the solution of the *m*PEG-*b*-PTFGE block copolymer, and the mixture was stirred for 30 min at room temperature. Subsequently, a total of 5 mL of deionized water was added to the solution at a rate of 0.5 mL min^{-1} using a syringe pump. It should be noted that the final concentration of pyrene (0.01 mg L^{-1}) is lower than the solubility of pyrene (0.135 mg L^{-1} at 25 °C).[19] The solution was left to equilibrate overnight. The fluorescence of each pyrene-containing polymer micelle solution (with different concentrations) was measured at an emission wavelength of 372 nm using a fluorometer in a 1 × 1 cm quartz cell. The following parameters were chosen: emission wavelength = 372 nm, excitation wavelength range = 300−360 nm, and data interval = 0.5 nm. The ratio of the fluorescence intensities at wavelengths of 339 and 332 nm was plotted versus the polymer concentrations, and the CMC was determined from the inflection point.

Pyrene Release Experiments. For the degradation kinetic studies, a buffer solution at pH 5.0 was prepared using sodium acetate/acetic acid, and a pyrene-containing polymeric micelle solution was prepared according to the procedure described in the CMC study above. Then, 0.10 mL of the pyrene-containing micelle solution was slowly added to 0.90 mL of the buffer solution and the changes in the excitation spectra were recorded.

In Vitro Cell Viability Assay. HeLa cells were grown in Dulbecco's modified Eagle's medium containing 10% fetal bovine

DOI: 10.1021/acs.macromol.9b00823
Macromolecules XXXX, XXX, XXX−XXX

serum (FBS) and 1% penicillin−streptomycin (10 000 U mL^{-1}), and HULEC-5a cells were grown in MCDB131 (without L-glutamine) containing 10 ng mL^{-1} epidermal growth factor, 1 μg mL−1 hydrocortisone, 10 mM glutamine, and FBS to a final concentration of 10%. HeLa and HULEC-5a cells were cultured in a humidified incubator at 37 °C with 5% CO_2. Cell viability for the F series was quantified by MTT assay [MTT = 3-(4,5-dimethyl-2-thiazolyl)-2,5-diphenyl-2*H*-tetrazolium bromide]. Cells were seeded in a 96-well plate at a concentration of 1.5 × 10^5 cells per mL and incubated overnight. Then, F series micelles of different concentrations (15, 30, 60, 125, 250, and 500 μg mL^{-1}, final 1% PBS) were added into the cell culture media, and the cells were incubated for an additional 24 h at 37 °C with 5% CO_2 in the dark. MTT (25 μL with 5 mg mL^{-1} PBS, pH 7.4) was added to each well, and cells were further incubated for 3 h. The old medium containing unreacted MTT was removed carefully, and formazan produced by living cells was dissolved in solubilization buffer [DMF (50% v/v), sodium dodecyl sulfate (10% w/v), 99.9% AcOH (0.4% v/v), and 1 N HCl (0.4% v/v)] overnight at room temperature. The absorbance (λ = 570 nm) was measured using a SpectraMax M5 microplate reader (Molecular Devices, Sunnyvale, CA). Cell viability was then determined relative to the control condition (average value of the absorbance of cells containing 1% of PBS).

Computational Details. All calculations are performed with the B3LYP/6-31G* level of theory as implemented in Gaussian09 program package.[20] Solvent effects are considered with polarizable continuum model for water parameters in addition to explicit water molecules. Molecular structures for several important reaction coordinates are given at the end of the Supporting Information (Tables S1−S6).

RESULTS AND DISCUSSION

Computational Analysis for Hydrolysis of Model Compounds: QM Calculation. Before exploring the degradation of the polymeric micelles with different types of acetal groups, we used a series of model compounds to accessing the hydrolysis kinetics of different acetal groups. Considering the potential effects of the ring-opening reaction of the epoxide group on the hydrolysis of the acetal group, we synthesized the following three model compounds: ethoxyethyl propyl ether (EEPE), tetrahydrofuranyl propyl ether (TFPE), and tetrahydropyranyl propyl ether (TPPE) (see Experimental Section for details).

To provide mechanistic insights into the hydrolysis of these model compounds, we performed computational analyses using a density functional theory approach (Figure 1). Specifically, 10 explicit water molecules (10 H_2O) and an additional proton (H^+) were included to calculate the reaction energy barriers. We note that we could not obtain a stable protonated form with a small number of explicit water molecules (i.e., proper solvation of protonated EEPE/TFPE/TPPE was critical for EEPE/TFPE/TPPE to be stabilized). First, optimized structures of the model acetal compounds before and after the protonation steps were obtained, including transition states (i.e., M + H_3O^+ + (9H_2O) → H^+ − M + 10H_2O; M = model compound). Reactants and products were optimized with the lowest-energy structures for several configurations, and the transition state between the two structures was obtained. Interestingly, we observed that an additional proton was attached to the inner shell of water molecules for both EEPE (acyclic; four carbons) and TFPE (cyclic; four carbons, 5-membered ring), whereas it was attached to the outer shell in the case of TPPE (cyclic; five carbons, 6-membered ring), suggesting enhanced hydrophobicity of TPPE compared to EEPE and TFPE (Figure S1).

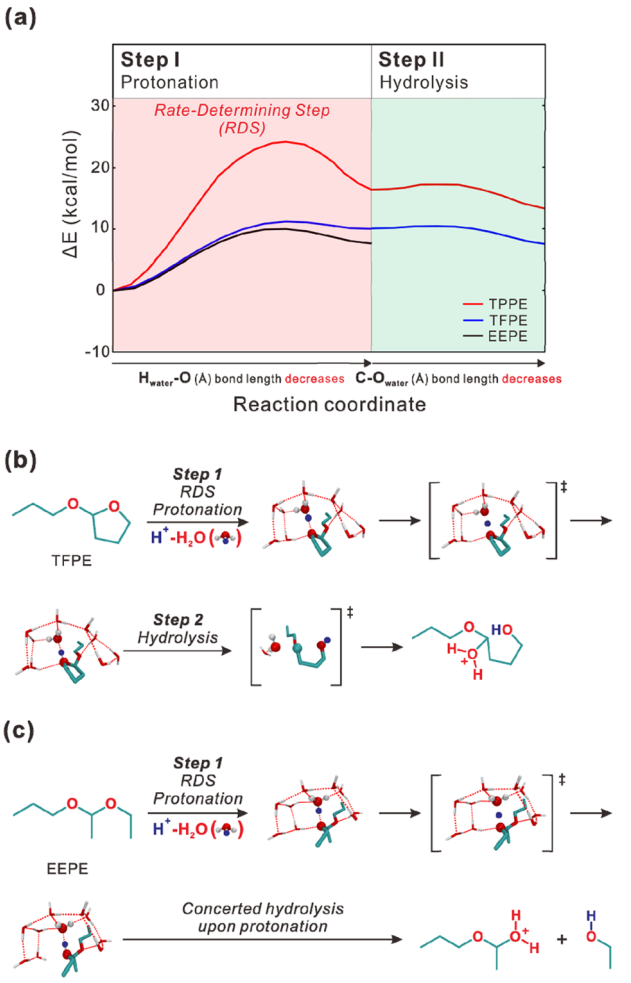

Figure 1. (a) Energy diagram of the hydrolysis reaction coordinates of the model acetal monomers, (b) proposed hydrolysis mechanisms of TFPE, and (c) ethoxyethyl propyl ether (EEPE) model compounds based on computational analysis. Note that the hydrolysis of TPPE is expected to proceed via an identical mechanism to that shown for TFPE (red: oxygen; white: hydrogen; blue: additional proton; green: carbon; the dashed lines represent the hydrogen-bonding networks of water).

Subsequently, the reaction energy barrier (ΔE) was calculated with a constrained optimization along a fixed distance between the proton and the oxygen in the cyclic structures of TFPE and TPPE (or the corresponding oxygen for EEPE). Reaction energy profiles are shown for the protonation of respective acetal model compounds (i.e., EEPE, TFPE, and TPPE) as a function of O−H bond length (Figure S2). Apparently, TPPE (24.2 kcal mol^{-1}) required a significantly higher reaction energy than TFPE (11.2 kcal mol^{-1}) or EEPE (10.0 kcal mol^{-1}) since two hydrogen-bond networks were involved in the protonation step of TPPE, whereas only one hydrogen bond was involved for EEPE and TFPE.

In general, the overall hydrolysis of the acetal linkages involves two steps: (1) a protonation step and (2) a bond cleavage step. The rate-determining step for the overall hydrolysis was the protonation reaction, with an energy barrier of 10.0−24.2 kcal mol^{-1}. It should be noted that both cyclic acetal compounds, TFPE and TPPE, followed a two-step process, whereas EEPE underwent a single-step, concerted

DOI: 10.1021/acs.macromol.9b00823
Macromolecules XXXX, XXX, XXX−XXX

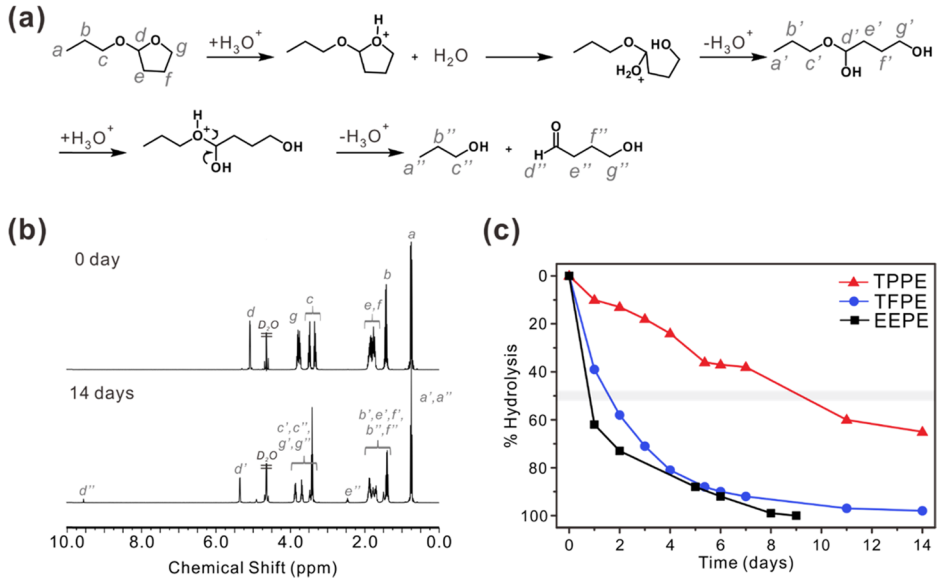

Figure 2. (a) Hydrolysis mechanism, (b) ^{1}H NMR spectra before and after hydrolysis of TFPE model compound (see Figure S4 for EEPE and TPPE), and (c) percentage hydrolysis rate of all model compounds determined by ^{1}H NMR spectra.

Scheme 2. (a) Design and Synthesis of TFGE Epoxide Monomer, (b) Block Copolymerization of TFGE with *m*PEG Macroinitiator by AROP, and (c) Structures of *m*PEG-*b*-PTPGE and *m*PEG-*b*-PEEGE[a]

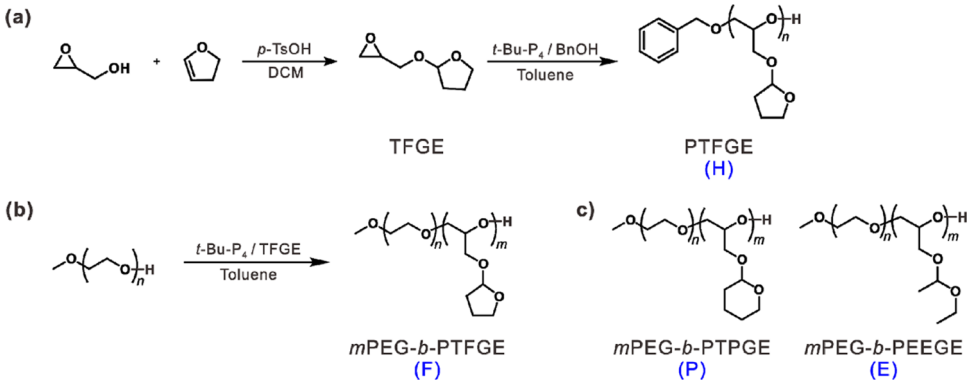

[a]Note that polymer code used in Table 1 for the corresponding polymer composition.

hydrolysis in which the protonation and bond cleavage occurred at the same time.

Subsequently, we calculated the transition state and reaction energy barrier for the hydrolysis step (protonated ring-opening) of the protonated TFPE and TPPE compounds (i.e., H$^+$-TFPE and H$^+$-TPPE; Figure 1b) with two explicit water molecules and for the hydrolysis of the protonated EEPE compound (i.e., H$^+$-EEPE; Figure 1c). In the case of H$^+$-EEPE, no reaction energy barrier was observed for C−O bond breaking, indicating that hydrolysis occurred spontaneously following the protonation reaction. However, the ring opening of H$^+$-TFPE and H$^+$-TPPE showed a transition state, even though the energy barrier was small ($\Delta E \sim 0.37$ kcal mol^{-1} and $\Delta E \sim 0.83$ kcal mol^{-1} for TFPE and TPPE, respectively) compared to that of the protonation step. The minimum-energy pathways for the ring-opening steps of both H$^+$-TFPE and H$^+$-TPPE displayed relatively low energy barriers (Figure S3).

Chemical Analysis for Hydrolysis of Model Compounds. The hydrolysis of the model compounds was monitored by ^{1}H NMR spectroscopy for 2 weeks under sodium acetate/acetic acid buffer at pH 5.0 (Figure 2). For example, the methine peak of TFPE (a, 5.24 ppm) disappeared after 14 days, whereas a new methine peak of intermediate diol (a′, 5.51 ppm) and aldehyde peak of product (d, 9.71 ppm) appeared (see Figure S4 for the hydrolysis of other model compounds). Moreover, the hydrolysis kinetics of model compounds was evaluated by integration of the reduced methine peak (a) with respect to the unchanged methyl peak of propyl group (c). From these analyses, a half-life of the hydrolysis for each model compound could be estimated using first-order reaction equations (Figure S5; 2.47 days for TFPE, 8.56 days for TPPE, and 1.43 days for EEPE). Consequently, the newly designed acetal-based 5-membered cyclic group (TFPE) was hydrolyzed much faster than the 6-membered cyclic group (TPPE), despite having a similar cyclic structure and number of carbons. Moreover, while the hydrolysis rate of TFPE was similar to that of the flexible acyclic open chain (EEPE), the two cases involved markedly different hydrolysis mechanisms (i.e., two steps for TFPE and one step for EEPE). Consistent with the theoretical evaluation by quantum mechanical calculations, this ^{1}H NMR-based kinetic study supported the importance of structural design of monomers in controlling the hydrolysis profile.

DOI: 10.1021/acs.macromol.9b00823
Macromolecules XXXX, XXX, XXX−XXX

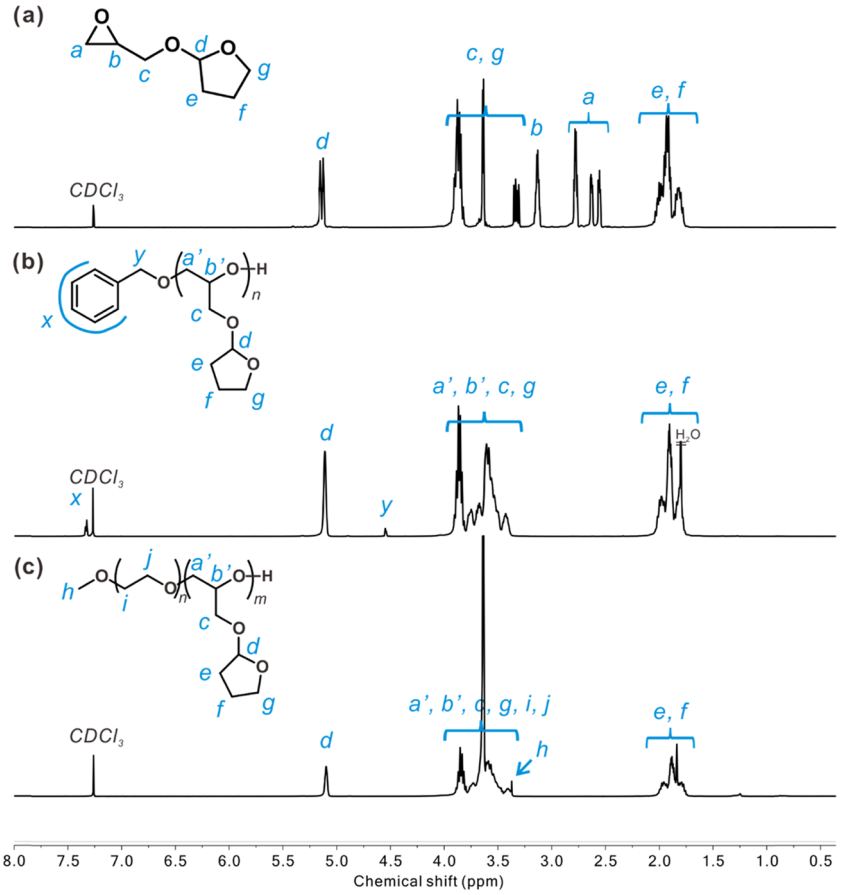

Figure 3. Representative ^{1}H NMR spectra of (a) the TFGE monomer, (b) the PTFGE homopolymer (H42), and (c) the *m*PEG-*b*-PTFGE block copolymer (F47).

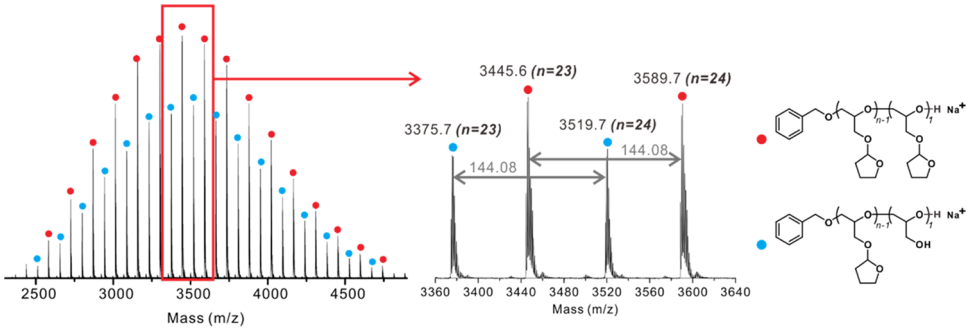

Figure 4. Representative MALDI-TOF mass spectrum of H32 homopolymer from 2300 to 4900 Da.

Design of Cyclic 5-Membered Epoxide Monomer and Synthesis of Amphiphilic Diblock Copolymers. A pH-responsive monomer (TFGE) was synthesized in a facile one-step reaction based on the reaction of glycidol and 2,3-dihydrofuran (Scheme 2). It was purified by fractional distillation, with a typical isolated yield of 75%. The chemical structure of TFGE was successfully defined using various NMR spectroscopic techniques, including ^{1}H, ^{13}C, correlation spectroscopy (COSY), and heteronuclear single-quantum correlation (HSQC), as well as mass spectrometry (Figures 3a and S6–S9). The purity of TFGE was more than 98%, as determined by gas chromatography–mass spectrometry (GC–MS) (Figure S10).

Amphiphilic diblock copolymers consisting of *m*PEG as the hydrophilic segment and poly(tetrahydrofuranyl glycidyl ether) (PTFGE) as the hydrophobic compartment were designed. Thus, the polymerization of the TFGE epoxide monomer was first optimized to achieve block copolymerization via AROP with benzyl alcohol as an initiator and *t*-BuP_4 as an organic superbase at room temperature. The organic superbase *t*-BuP_4 was chosen as it enables the controlled polymerization of PTFGE homopolymers under mild conditions.[21−23] The homopolymers were characterized by ^{1}H NMR, GPC, DSC, and MALDI-TOF mass spectrometry techniques (Figures 3, 4, and S11). The polymerizations were well controlled to give PTFGEs of narrow molecular weight distributions with the desired molecular weight (H32: conversion > 99%, $M_{n,\,GPC}$ = 3800, M_w/M_n = 1.08; H42: conversion > 99%, $M_{n,\,GPC}$ = 4500, M_w/M_n = 1.08; Table 1 and Figure S11).

DOI: 10.1021/acs.macromol.9b00823
Macromolecules XXXX, XXX, XXX−XXX

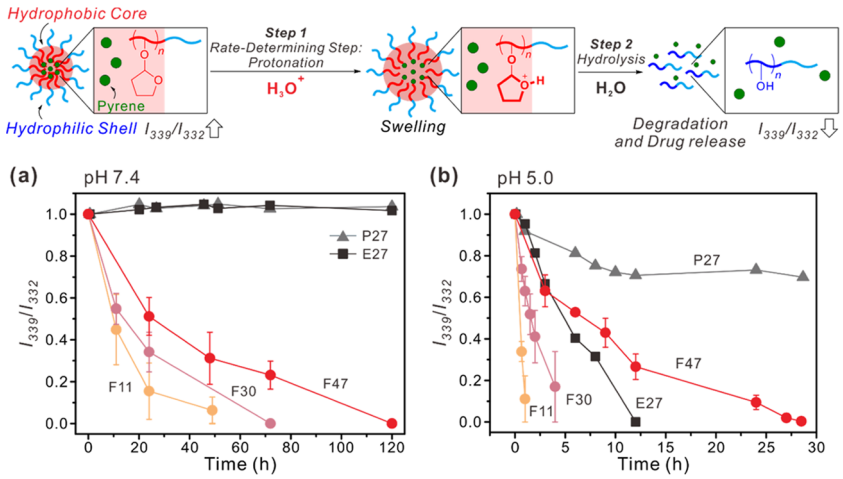

Figure 5. Drug-release profiles of pyrene-loaded micelles at (a) pH 7.4 and (b) pH 5.0. Note that the data for E27 and P27 are reproduced from our previous report.[18]

As shown in Figure 3, the structural properties of the obtained polymers were characterized by ^{1}H NMR spectroscopy. For example, the disappearance of the epoxide peaks (a and b; 2.50−3.20 ppm; Figure 3a) indicated the successful polymerization of TFGE monomers. Furthermore, the other peaks were clearly assigned: aromatic protons (x; 7.30−7.34 ppm), methine proton (d; 5.07−5.13 ppm), benzylic protons (y; 4.51−4.55 ppm), polyether backbone protons (a′, b′, and c; 3.34−3.92 ppm), and tetrahydrofuranyl protons (e, f, and g; 1.70−2.03 ppm). The theoretical number-average molecular weight ($M_{n,NMR}$) was calculated using the integration of two peaks: benzylic protons (y) from the initiator and the methine proton (d) from side groups (H32, $M_{n,NMR}$ = 4700; H42, $M_{n,NMR}$ = 6200).

To confirm the presence of benzyl alcohol and the successful incorporation of TFGE into the PTFGE homopolymer, the MALDI-TOF spectrum was acquired (Figure 4). The molecular weight of 3445.6 g mol^{-1} corresponded to a homopolymer chain with a benzyl alcohol initiator (108.06 g mol^{-1}), 23 monomer units (144.08 g mol^{-1}), and Na^+ as a counter cation. Interestingly, minor peaks with regular spacing were observed, possibly resulting from the degradation of the tetrahydrofuranyl group (71.05 g mol^{-1}) by the strong laser intensity. The spacing between two major peaks or two minor peaks corresponded to the molecular weight of the repeating unit, proving the successful polymerization.

In the subsequent step, block copolymerization using *m*PEG-OH as a hydrophilic macroinitiator was performed. A series of PEG-*b*-PTFGE amphiphilic block copolymers with different lengths of hydrophobic PTFGE chain were prepared to control the hydrophobicity and characterized by ^{1}H NMR, GPC, and DSC analyses (Figures 3c and S12). As clearly shown in Figure 3c, the ^{1}H NMR spectrum of the block copolymer displayed characteristic proton peaks: the methyl group of the *m*PEG macroinitiator (h; 3.37 ppm), tetrahydrofuranyl side chains (d; 5.05−5.16 ppm and e, f, and g; 1.74−2.02 ppm), and the polyether backbone (i and j; 3.35−3.94 ppm). The degree of polymerization of the block copolymers was calculated by integrating two peaks: the methyl proton (h) of *m*PEG and the methine proton (d) of the tetrahydrofuranyl group. In concert with the ^{1}H NMR data, the GPC results of the copolymers indicated monomodal distributions with a narrow dispersity (M_w/M_n < 1.07) in all cases (Table 1).

DSC studies provided the glass-transition temperatures (T_g) of a series of *m*PEG-*b*-PTFGE block copolymers (Table 1 and Figure S12). With increasing degree of polymerization of TFGE on the *m*PEG-*b*-PTFGE, T_g increased from −35 °C (F11) to −28 °C (F47). In comparison to the amphiphilic block copolymers previously synthesized from other monomers such as EEGE and TPGE, the T_g values of the TFGE series were higher than that of E27 (−59 °C). This was attributed to the presence of the rigid cyclic structure of TFGE. The T_g of P27 (−18 °C) made from TPGE monomers, however, was higher than that of F30 (−29 °C), owing to the bulky pendant group. These results suggest that the rigid cyclic structures of TFGE and TPGE assist the packing of block copolymers. Interestingly, all copolymers exhibited a single T_g, indicating that the block copolymers consisted exclusively of the polyether backbone.[24,25]

Self-Assembly Behavior of Amphiphilic Block Copolymers. The size control of self-assembled polymeric micelles is important to apply as drug-delivery carrier in human body for their circulation time and distribution.[26] Thus, the evaluation of critical micelle concentration (CMC) for obtained polymers was first performed by fluorimeter using pyrene as a fluorescent probe to investigate their self-assembly behavior and stability of micelles.[27,28] By taking advantage of the unique environment-sensitive fluorescence of pyrene within the hydrophobic core of micelles, we plotted I_{339}/I_{332} (intensity of 339 over 332 nm) as a function of polymer concentration to obtain a CMC value. The estimated CMC values of the polymers were 626.7 (F11), 150.6 (F30), and 113.6 mg L^{-1} (F47) (Table 1 and Figures S13 and S14). These CMCs were generally higher than those of the other polymers, E27 (76.7 mg L^{-1}) and P27 (10.9 mg L^{-1}), from EEGE and TPGE monomers. This could be attributed to the low hydrophobicity of the TFGE monomer since an increase in hydrophobicity could cause a decrease in the CMC value.[29] Meanwhile, the hydrophobicity of monomers could be estimated using the partition coefficient (log *P*) with a computational model, ALOGPS 2.1; the calculated log *P* values were 0.25 (TFGE), 0.45 (EEGE), and 0.66 (TPGE).[30]

The size and shape of micelles were also determined via DLS at the concentration above CMC value (5 mg mL^{-1}). Three

DOI: 10.1021/acs.macromol.9b00823
Macromolecules XXXX, XXX, XXX−XXX

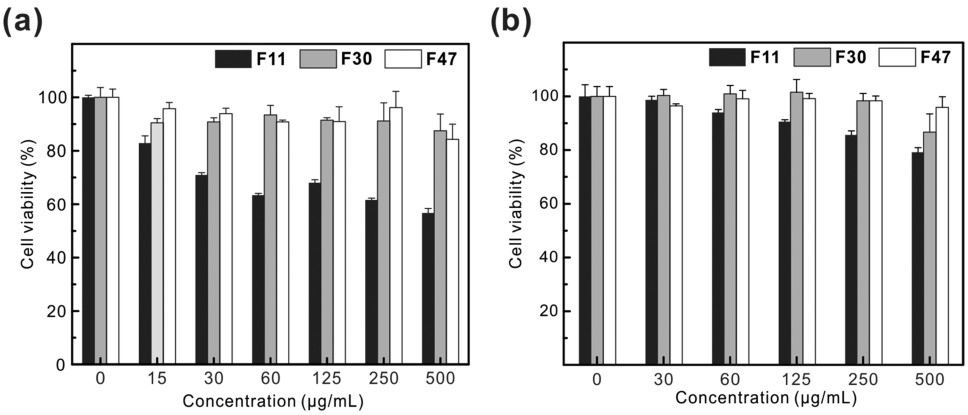

Figure 6. In vitro cell viability assay of block copolymer micelles determined by the MTT assay using (a) HeLa cells and (b) HULEC-5a cells.

copolymers carrying different chain lengths of the PTFGE block in amphiphilic block copolymers (F series) were employed to determine the average micelle sizes. While the hydrodynamic radius (R_h) of F11 was not determined clearly due to the presence of large aggregates, the size of the polymeric micelles decreased with increasing hydrophobicity, for example, 42.8 nm for F30 and 14.1 nm for F47. Moreover, the morphology of the representative F47 micelle was observed with AFM. The AFM image yielded a spherical shape of the micelles with a relatively uniform size distribution (R_h = 30.9 ± 2.0 nm) in concert with the observation by DLS (Figure S15).

The encapsulation efficiency is another important factor for drug-delivery carriers. Here, we investigated the encapsulation efficiency using a model hydrophobic dye, Nile Red, within the core of the micelles. The loading efficiencies of Nile Red into micelles made from the respective block copolymers were 4.7% (F11), 8.5% (F30), and 9.8% (F47) (Figure S16). Compared to the loading efficiency of other different series, 6.4% (E27) and 25.9% (P27), indicated that the less hydrophobic micellar core consisting of TFGE did not result in a significant driving force for the formation of micelles and encapsulation of the model drug.

Stability of Polymeric Micelles and Degradation Kinetics. The stability of the encapsulated polymeric micelle is important for delivery of the therapeutic materials to the target cell, as well as for temporal control of the release of the drug over an extended period of time or for a specific duration during treatment. Thus, the stability of pyrene-encapsulated polymeric micelles (F series) compared to that of other polymeric micelles (E27 and P27) under neutral conditions was monitored by measuring the change in the I_{339}/I_{332} ratio in the excitation spectra of pyrene (Figure 5a). The F11, F30, and F47 polymeric micelles were less stable compared to the other polymeric micelles (E27 and P27). The stability of the micelles in PBS was also highly dependent on the hydrophobicity of the amphiphilic block copolymer (P27 ≈ E27 (> 120 h) ≫ F47 (120 h) > F30 (72 h) > F11 (47 h)). This trend was consistent with the obtained CMC values of the micelles, showing that a polymeric micelle with a lower CMC value (indicating higher hydrophobicity) would form a more densely packed hydrophobic core at a given concentration. Nevertheless, the integrity of the F series of polymeric micelles remained over 80% after 10 h, indicating that it could be suitable for use as a drug-delivery carrier.[31]

Next, we evaluated the degradation of the micelles at pH 5.0. The acetal pendant groups in the hydrophobic core of the polymeric micelles were cleaved in the acidic environment, and the hydrophobic blocks in the core were gradually converted into hydrophilic linear polyglycerol blocks, eventually leading to the degradation of micelles followed by the release of the pyrene (Figure 5b). The release rates of the F series micelles at pH 5.0 were clearly higher than those at pH 7.4, owing to enhanced hydrolysis. In general, the complete degradation times for F series micelles were 1 h (F11), 4 h (F30), and 29 h (F47), indicating the potential to control degradation over a wide time frame by adjusting the hydrophilicity−hydrophobicity balance. Moreover, the micelles composed of the polymer F30 showed more rapid degradation (4 h) than others with a similar degree of hydrophobic block polymerization, for example, E27 (12 h) and P27 (>30 h). This was because micelles formed from the F30 polymer, which had the highest CMC value, formed a more loosely packed micellar core at a given concentration, allowing the acid to penetrate more readily into the micelle core. Moreover, it should be noted that all micelles were degraded into a highly biocompatible double hydrophilic block copolymer that could be readily cleared from the body.

Overall, the chemical structures of the monomers, which were correlated with both hydrophobicity and degradability, led to the different degradation kinetics observed between the monomers and the corresponding micelles. Although the TFGE model compound showed an intermediate level of degradability, the corresponding micelle had a relatively high degradation rate. We postulate that the cyclic moiety is a key factor for hydrolysis rate of monomers; thus, it led to a two-step hydrolysis while acyclic monomer shows a one-step hydrolysis. On the other hand, hydrophobicity is more critical in determining both stability of micelles and packing density in the micelle core. The loose packing of the F series micelles due to their higher CMC values indicates that their hydrophobic core is more easily protonated; thus, they are degraded more rapidly than the compactly packed micelles with low CMC values.

Cell Viability of the Polymeric Micelles. Micelles used in drug-delivery system should be highly biocompatibility to minimize the toxicity of drugs during blood circulation to target cells. To confirm the pharmaceutical applicability of all of the polymers we prepared, the viabilities of human cervical cancer cells (HeLa) and human lung microvascular endothelial cells (HULEC-5a) were investigated by MTT assay (Figure 6). The results showed that F30 and F47 were suitable for application in drug-delivery system as both HeLa and HULEC-

DOI: 10.1021/acs.macromol.9b00823
Macromolecules XXXX, XXX, XXX−XXX

5a cells retained viabilities of approximately 100% when exposed to concentrations of 500 μg mL^{-1}. On the contrary, cell viability with F11 was relatively low, possibly owing to its high CMC value (626.7 mg L^{-1}), as the exposed hydrophobic block could interfere with the cellular membrane. In particular, HeLa cells are known to be more sensitive to the toxicity of the amphiphiles like F11 compared to well-ordered polarized cell lines because of its nonpolarized and less-ordered cellular membranes.[32] In conclusion, F30 and F47 among the F series are suitable for DDS, owing to their high biocompatibility toward both cancerous and normal vascular cells in hydrophilic micelle formation.

CONCLUSIONS

In conclusion, we designed a new epoxide monomer, TFGE, for smart drug delivery in a site-specific and time-controlled manner. First, the new monomer was examined using both experimental and computational methods and compared to previously reported epoxide model monomers, namely, EEPE and TPPE, with respect to hydrolysis rate. The model monomers with cyclic moieties (TFPE and TPPE) involved a two-step hydrolysis mechanism, while that with an acyclic moiety (EEPE) involved a one-step hydrolysis mechanism. This resulted in TFGE having a lower hydrolysis rate than EEGE, despite the two monomers consisting of the same number of carbons. Furthermore, TFPE was hydrolyzed faster than TPPE because the lower hydrophobicity of TFPE meant it had a lower energy barrier for protonation. Moreover, a series of amphiphilic block copolymers, *m*PEG-*b*-PTFGE, were obtained by AROP using *m*PEG and *t*-BuP_4 as a macroinitiator and an organic superbase, respectively. Various properties of micelles composed of *m*PEG-*b*-PTFGE polymers were studied, including their CMC, encapsulation efficiency, drug-release behavior, and effects on cell viability. The CMC values of *m*PEG-*b*-PTFGE polymers were higher than those of *m*PEG-*b*-PEEGE and *m*PEG-*b*-PTPGE polymers, which was ascribed to the lower hydrophobicity of tetrahydrofuranyl group compared to the ethoxyethyl or tetrahydropyranyl group. Interestingly, the micelle composed of *m*PEG-*b*-PTFGE was degraded most rapidly, followed by the micelles made of *m*PEG-*b*-PEEGE and *m*PEG-*b*-PTPGE, even though the model compounds of EEGE and TFGE showed similar hydrolysis rates. This confirmed that hydrophobicity is an especially significant factor for micelle stability, loading efficiency, and even drug-release behavior. Finally, we demonstrated the nontoxicity of the micelles for potential pharmaceutical applications in the human body.

ASSOCIATED CONTENT

Supporting Information

The Supporting Information is available free of charge on the ACS Publications website at DOI: 10.1021/acs.macromol.9b00823.

Potential energy profiles, NMR, MS, GC−MS, GPC, DSC, CMC, DLS, AFM, and encapsulation efficiencies of micelles (PDF)

AUTHOR INFORMATION

Corresponding Authors

*E-mail: slee@krict.re.kr (S.-H.L.).
*E-mail: skmin@unist.ac.kr (S.K.M.).
*E-mail: bskim19@yonsei.ac.kr (B.-S.K.).

ORCID

Eunbyul Hwang: 0000-0001-5130-7940
Tae-Hyuk Kwon: 0000-0002-1633-6065
Sang-Ho Lee: 0000-0003-2207-3369
Seung Kyu Min: 0000-0001-5636-3407
Byeong-Su Kim: 0000-0002-6419-3054

Notes

The authors declare no competing financial interest.

ACKNOWLEDGMENTS

The authors thank Tae-young Heo in Hongik University for useful comments and measurement of DLS, and Dongseok Kim in Yonsei University for measurement of AFM. This work was supported by the National Research Foundation of Korea (NRF-2017R1A2B3012148). C.G.L. acknowledges the support from the Global Ph.D. fellowship program through the National Research Foundation of Korea (NRF) (NRF-2018H1A2A1061237).

REFERENCES

(1) Du, J.-Z.; Sun, T.-M.; Song, W.-J.; Wu, J.; Wang, J. A Tumor-Acidity-Activated Charge-Conversional Nanogel as an Intelligent Vehicle for Promoted Tumoral-Cell Uptake and Drug Delivery. *Angew. Chem., Int. Ed.* **2010**, *122*, 3703−3708.

(2) Lee, S.-M.; Chen, H.; Dettmer, C. M.; O'Halloran, T. V.; Nguyen, S. T. Polymer-Caged Lipsomes: A pH-Responsive Delivery System with High Stability. *J. Am. Chem. Soc.* **2007**, *129*, 15096−15097.

(3) Kim, B.-S.; Lee, H.-I.; Min, Y.; Poon, Z.; Hammond, P. T. Hydrogen-Bonded Multilayer of pH-Responsive Polymeric Micelles with Tannic Acid for Surface Drug Delivery. *Chem. Commun.* **2009**, *293*, 4194−4196.

(4) Owen, S. C.; Chan, D. P. Y.; Shoichet, M. S. Polymeric Micelle Stability. *Nano Today* **2012**, *7*, 53−65.

(5) Slor, G.; Papo, N.; Hananel, U.; Amir, R. J. Tuning the Molecular Weight of Polymeric Amphiphiles as a Tool to Access Micelles with a Wide Range of Enzymatic Degradation Rates. *Chem. Commun.* **2018**, *54*, 6875−6878.

(6) Zhao, X.; Poon, Z.; Engler, A. C.; Bonner, D. K.; Hammond, P. T. Enhanced Stability of Polymeric Micelles Based on Postfunctionalized Poly(Ethylene Glycol)-*b*-Poly(γ-Propargyl L-Glutamate): The Substituent Effect. *Biomacromolecules* **2012**, *13*, 1315−1322.

(7) Ma, C.; Pan, P.; Shan, G.; Bao, Y.; Fujita, M.; Maeda, M. Core−Shell Structure, Biodegradation, and Drug Release Behavior of Poly(Lactic Acid)/Poly(Ethylene Glycol) Block Copolymer Micelles Tuned by Macromolecular Stereostructure. *Langmuir* **2015**, *31*, 1527−1536.

(8) Glavas, L.; Olsén, P.; Odelius, K.; Albertsson, A.-C. Achieving Micelle Control through Core Crystallinity. *Biomacromolecules* **2013**, *14*, 4150−4156.

(9) Gou, J.; Feng, S.; Xu, H.; Fang, G.; Chao, Y.; Zhang, Y.; Xu, H.; Tang, X. Decreased Core Crystallinity Facilitated Drug Loading in Polymeric Micelles without Affecting Their Biological Performances. *Biomacromolecules* **2015**, *16*, 2920−2929.

(10) Meng, F.; Zhong, Z.; Feijen, J. Stimuli-Responsive Polymersomes for Programmed Drug Delivery. *Biomacromolecules* **2009**, *10*, 197−209.

(11) Son, S.; Shin, E.; Kim, B.-S. Light-Responsive Micelles of Spiropyran Initiated Hyperbranched Polyglycerol for Smart Drug Delivery. *Biomacromolecules* **2014**, *15*, 628−634.

(12) Seidi, F.; Jenjob, R.; Crespy, D. Designing Smart Polymer Conjugates for Controlled Release of Payloads. *Chem. Rev.* **2018**, *118*, 3965−4036.

(13) D'Souza, A. J. M.; Topp, E. M. Release from Polymeric Prodrugs: Linkages and Their Degradation. *J. Pharm. Sci.* **2004**, *93*, 1962−1979.

DOI: 10.1021/acs.macromol.9b00823
Macromolecules XXXX, XXX, XXX−XXX

(14) Morinaga, H.; Morikawa, H.; Wang, Y.; Sudo, A.; Endo, T. Amphiphilic Copolymer Having Acid-Labile Acetal in the Side Chain as a Hydrophobe: Controlled Release of Aldehyde by Thermoresponsive Aggregation-Dissociation of Polymer Micelles. *Macromolecules* **2009**, *42*, 2229−2235.
(15) Shenoi, R. A.; Narayanannair, J. K.; Hamilton, J. L.; Lai, B. F. L.; Horte, S.; Kainthan, R. K.; Varghese, J. P.; Rajeev, K. G.; Manoharan, M.; Kizhakkedathu, J. N. Branched Multifunctional Polyether Polyketals: Variation of Ketal Group Structure Enables Unprecedented Control over Polymer Degradation in Solution and within Cells. *J. Am. Chem. Soc.* **2012**, *134*, 14945−14957.
(16) Huang, F.; Cheng, R.; Meng, F.; Deng, C.; Zhong, Z. Micelles Based on Acid Degradable Poly(Acetal Urethane): Preparation, pH-Sensitivity, and Triggered Intracellular Drug Release. *Biomacromolecules* **2015**, *16*, 2228−2236.
(17) Song, J.; Palanikumar, L.; Choi, Y.; Kim, I.; Heo, T.; Ahn, E.; Choi, S.-H.; Lee, E.; Shibasaki, Y.; Ryu, J.-H.; Kim, B.-S. The Power of the Ring: A pH-Responsive Hydrophobic Epoxide Monomer for Superior Micelle Stability. *Polym. Chem* **2017**, *8*, 7119−7132.
(18) Song, J.; Hwang, E.; Lee, Y.; Palanikumar, L.; Choi, S.-H.; Ryu, J.-H.; Kim, B.-S. Tailorable Degradation of pH-Responsive All Polyether Micelles via Copolymerisation with Varying Acetal Groups. *Polym. Chem.* **2019**, *10*, 582−592.
(19) Miller, M. M.; Wasik, S. P.; Huang, G. L.; Shiu, W. Y.; Mackay, D. Relationships Between Octanol-Water Partition Coefficient and Aqueous Solubility. *Environ. Sci. Technol.* **1985**, *19*, 522−529.
(20) Frisch, M. J.; Trucks, G. W.; Schlegel, H. B.;et al. *Gaussian 09*, revision A.02; Gaussian, Inc.: Wallingford, CT, 2009.
(21) Förster, S.; Krämer, E. Synthesis of PB−PEO and PI−PEO Block Copolymers with Alkyllithium Initiators and the Phosphazene Base *t*-BuP_4. *Macromolecules* **1999**, *32*, 2783−2785.
(22) Satoh, Y.; Miyachi, K.; Matsuno, H.; Isono, T.; Tajima, K.; Kakuchi, T.; Satoh, T. Synthesis of Well-Defined Amphiphilic Star-Block and Miktoarm Star Copolyethers via *t*-Bu-P_4 -Catalyzed Ring-Opening Polymerization of Glycidyl Ethers. *Macromolecules* **2016**, *49*, 499−509.
(23) Pietzonka, T.; Seebach, D. The P4-Phosphazene Base as Part of a New Metal-Free Initiator System for the Anionic Polymerization of Methyl Methacrylate. *Angew. Chem., Int. Ed.* **1993**, *32*, 716−717.
(24) Xu, Y.; He, Y.; Wei, J.; Fan, Z.; Li, S. Morphology and Melt Crystallization of PCL-PEG Diblock Copolymers. *Macromol. Chem. Phys.* **2008**, *209*, 1836−1844.
(25) Jadhav, N.; Gaikwad, V.; Nair, K.; Kadam, H. Glass Transition Temperature: Basics and Application in Pharmaceutical Sector. *Asian J. Pharm.* **2009**, *3*, 82−89.
(26) Stolnik, S.; Illum, L.; Davis, S. S. Long Circulating Microparticulate Drug Carriers. *Adv. Drug Delivery Rev.* **1995**, *16*, 195−214.
(27) Wilhelm, M.; Zhao, C. L.; Wang, Y.; Xu, R.; Winnik, M.; Mura, J. L.; Riess, G.; Croucher, M. D. Poly(Styrene-Ethylene Oxide) Block Copolymer Micelle Formation in Water: A Fluorescence Probe Study. *Macromolecules* **1991**, *24*, 1033−1040.
(28) Jeong, Y.-H.; Shin, H.-W.; Kwon, J.-Y.; Lee, S.-M. Cisplatin-Encapsulated Polymeric Nanoparticles with Molecular Geometry-Regulated Colloidal Properties and Controlled Drug Release. *ACS Appl. Mater. Interfaces* **2018**, *10*, 23617−23629.
(29) Noda, T.; Hashidzume, A.; Morishima, Y. Effects of Spacer Length on the Side-Chain Micellization in Random Copolymers of Sodium 2-(Acrylamido)-2-Methylpropanesulfonate and Methacrylates Substituted with Ethylene Oxide-Based Surfactant Moieties. *Macromolecules* **2001**, *34*, 1308−1317.
(30) Tetko, I. V.; Gasteiger, J.; Todeschini, R.; Mauri, A.; Livingstone, D.; Ertl, P.; Palyulin, V. A.; Radchenko, E. V.; Zefirov, N. S.; Makarenko, A. S.; Tanchuk, V. Y.; Prokopenko, V. V. Virtual Computational Chemistry Laboratory-Design and Description. *J. Comput.-Aided Mol. Des.* **2005**, *19*, 453−463.
(31) Hu, Y.; Litwin, T.; Nagaraja, A. R.; Kwong, B.; Katz, J.; Watson, N.; Irvine, D. J. Cytosolic Delivery of Membrane-Impermeable Molecules in Dendritic Cells Using pH-Responsive Core−Shell Nanoparticles. *Nano Lett.* **2007**, *7*, 3056−3064.
(32) Inácio, A. S.; Mesquita, K. A.; Baptista, M.; Ramalho-Santos, J.; Vaz, W. L.; Vieira, O. V. In vitro Surfactant Structure-Toxicity Relationships: Implications for Surfactant Use in Sexually Transmitted Infection Prophylaxis and Contraception. *PLoS One* **2011**, *6*, No. e19850.

DOI: 10.1021/acs.macromol.9b00823
Macromolecules XXXX, XXX, XXX−XXX